SEMARAK ILMU PUBLISHING

Journal of Advanced Research in Applied Mechanics

Journal homepage:
https://semarakilmu.com.my/journals/index.php/appl_mech/index
ISSN: 2289-7895

The Effect of Implant Length and Bone Quality on the Biomechanical Responses of Dental Implant and Surrounding Bone – A Three-Dimensional Finite Element Analysis

Muhammad Ikman Ishak[1,*], Ruslizam Daud[1], Siti Noor Fazliah Mohd Noor[2], Khor Chu Yee[1], Husniyati Roslan[2]

[1] Fakulti Kejuruteraan & Teknologi Mekanikal, Universiti Malaysia Perlis (UniMAP), Kampus Alam UniMAP, Pauh Putra, 02600 Arau, Perlis, Malaysia
[2] Advanced Medical and Dental Institute, Universiti Sains Malaysia, Bertam, Jln. Tun Hamdan Sheikh Tahir, 13200 Kepala Batas, Pulau Pinang, Malaysia

ARTICLE INFO

Article history:
Received 14 February 2024
Received in revised form 11 April 2024
Accepted 25 April 2024
Available online 30 May 2024

Keywords:
Bone quality; deformation; dental implant; finite element analysis; implant length, stress

ABSTRACT

The robustness of dental implant systems in the context of occlusal restoration relies significantly on biomechanical factors associated with the imposition of excessive loads. These factors encompass the macro geometries of the implants, bone qualities, parafunctional oral habits, and specific materials employed. The choice of different implant lengths in different bone qualities may give rise to distinct effects on the way loads are distributed across the interface between the implant and the adjacent bone. As of now, the influence of implant length and bone quality on the surrounding tissues and the stability of implant structure continues to be a matter of debate and uncertainty, particularly in situations involving the possibility of implant failure. This study employed three-dimensional finite element analysis to investigate five distinct implant lengths (4, 6, 10, 13, and 15 mm) in two types of bone quality (type II and III). The bone tissues were characterized through the utilization of computed tomography image datasets and then underwent processing within the SolidWorks software. All geometric configurations were transformed into finite element models, which were subjected to analysis within the ANSYS software. Anisotropic and isotropic properties were attributed to the bone and implant models, respectively. A dynamic occlusal loading quantified at 300 N was applied to the implant body, accompanied by a pre-tension force of 20 N on the screw component. The longer implants exhibited decreased stress magnitudes in type II bone (87.86 – 36.66 MPa) and increased stress magnitudes in type III bone (80.5 – 2128.9 MPa) within the surrounding bone tissue, in comparison to the shorter implants. However, stress within the implant body was generally elevated with the use of longer implants in both bone types (type II: 505.32 – 625.35 MPa; type III: 500.45 – 2186.7 MPa). Irrespective of bone quality, the longer implants predominantly led to lower bone strain levels (type II: 0.006828 – 0.003328; type III: 0.054250 – 0.021678) and overall deformation of the implant-abutment assembly (type II: 0.1458 – 0.1348 µm; type III: 0.1754 – 0.1492 µm) compared to their shorter counterparts. Among all the assessed findings, type III bone displayed a more pronounced adverse impact on the biomechanical responses of the dental implant and neighbouring bone except for the implant stresses under the applied physiological loading.

* *Corresponding author.*
E-mail address: ikman@unimap.edu.my

https://doi.org/10.37934/aram.118.1.1327

1. Introduction

A dental implant system designed for replacing missing teeth is a commonly used dental implant in prosthodontics. It is placed in both soft and hard oral tissues to provide support for fixed or removable prostheses. Comprising three key components – abutment screw, abutment, and implant body – a standard osseointegrated dental implant is used to attach artificial teeth (like crowns) to the jawbone. This enables the distribution of biting and chewing forces and is among the best options to restore missing teeth in terms of comfort, function, and aesthetics. Numerous clinical follow-up studies have provided substantial evidence for the success of dental implants over the years [1,2]. Despite this, complications after implantation that lead to implant failures, such as abutment and implant body fractures and loosening, still exist. Although occurrences of implant body fractures are infrequent, comprising only 0.2 to 1.5% of cases [3], their consequences evoke significant distress among both dental surgeons and patients [4]. When an implant is lost, it necessitates maintenance and additional corrective measures, often involving a new rehabilitation period.

Implant complications arise from two main factors: technical overloading and biological-related incidents. Technical overloading has a more pronounced impact on implant stability than biological events. This can be attributed to various insufficient biomechanical aspects of the implant that weaken the bone-implant connection. The absence of periodontal ligaments further worsens this, as they are unable to provide support for physiological loads. An unusual response of the implant to loading can lead to marginal bone loss and subsequent failure of the prosthesis or implant components. Additionally, consequences include soft tissue distortion, compromised aesthetics, and patient dissatisfaction [5]. Given these concerns, it is vital to ensure that the interaction between bone and implant, influenced by biomechanical overloading factors, remains within acceptable physiological limits. Factors like the abutment height, implant material, length, diameter [3], cervical wall thickness of the implant body [6], parafunctional oral habits [7], and bone quantity and quality [8] are the most prevalent biomechanical overloading contributors known to induce implant unpredictability. Some studies have indicated that the nature of the load exerts a more pronounced influence, whereas in alternative research, bone quantity and quality are emphasized as the foremost determining factors [8]. Inadequate conditions can result in overloads, leading to peri-implant bone resorption or implant fatigue failure, while insufficient loading of the bone may trigger atrophy followed by subsequent bone loss [9].

The length of the implant is measured as the distance from the implant's platform to its apex. The implant's length is also linked to its total surface area. Lengthening the implant is thought to enhance the extent of contact between the implant and bone [10]. When selecting the suitable implant length, various factors are taken into account, including the patient's individual characteristics and the anatomical conditions of the specific site. The initial contact between bone and implant plays a crucial role in establishing the functional surface area, and this is largely influenced by the density of the bone. As outlined by Lekholm and Zarb, the classification of jawbone quality can be categorized into four primary groups – types I, II, III, and IV. Type 1 bone quality pertains to jaws that are made up of uniform, compact bone. In the case of type 2, the bone includes a central dense cancellous core encircled by a cortical bone layer measuring 2 mm in thickness. Type 3 bone features a slender cortical bone layer enveloping a core of densely packed cancellous bone, while type 4 bone is characterized by a fragile, low-density cancellous core enclosed by a thin cortical bone layer, indicating weak strength. Type 1 bone is infrequent and predominantly observed in the anterior mandibular region. Conversely, type 2 bone is the prevailing type, distributed widely across various regions of the mandible. Type 3 bone is frequently encountered in the anterior maxilla. Lastly, type 4 bone is predominantly identified in the posterior maxilla.

In implant dentistry, type I bone is reported to encourage around 80% bone-implant contact, whereas types II, III, and IV show lower percentages [11]. In addition to bone quality and quantity, the clinician's familiarity with diverse or novel implant designs can also impact the results. The impact of various implant lengths in different bone qualities on implant stability is a topic of ongoing discussion and lacks clarity. Additionally, there is a dearth of information concerning the appropriate choice of implant length in different bone qualities, which in turn underscores the importance of prioritizing implant design before proceeding with fabrication.

Currently, computational analysis holds a prominent and widely accepted method for investigating biomechanical characteristics, encompassing changes in stress and strain. It offers greater ease and flexibility compared to experimental testing. In dental implantology, finite element analysis (FEA) stands out as an extensively used computational technique. It empowers researchers to predict outcomes that can be challenging to ascertain through *in vitro* and *in vivo* studies, especially at the interface between bone and implant [12-14]. FEA plays a pivotal role in addressing mathematical modelling challenges across various scientific and industrial domains, spanning analyses like structural, vibration [15], manufacturing [16], fatigue, fluid [17-19], fracture mechanics, and thermal [20].

Therefore, the objective of this study was to assess the mechanical reactions of a dental implant, analyzing stress, strain, and deformation across five distinct implant lengths: 4, 6, 10, 13, and 15 mm, in two different bone qualities of the lower jawbone: type II and III, utilizing three-dimensional (3-D) finite element analysis (FEA). The null hypothesis posits that the variation in the implant length and bone quality lack significance in influencing biomechanical responses. It is anticipated that this investigation will enhance comprehension of load distribution at the bone-implant interface, thus addressing the concern of implant instability that often results in failure that related to implant length and bone quality. Moreover, deepening the comprehension of implants with different lengths within distinct bone structures could play a crucial role for clinicians when evaluating implant and bone specifications prior to the surgical placement of dental implants.

2. Materials and Methods

2.1 Construction of Three-Dimensional Mandibular Bone Model

A series of craniofacial computed tomography (CT) image datasets were utilized and subjected to analysis with the objective of constructing a three-dimensional (3D) model of the mandibular bone. The model was developed using image-processing software, specifically Mimics 20.0 (Materialise, Leuven, Belgium). In the context of this investigation, a single CT dataset from an actual craniofacial case was considered. The CT scan image datasets underwent processing using an appropriate bone density scale, facilitating the differentiation of cancellous and cortical bone structures. The specific area of focus was the posterior segment of the left mandible, encompassing regions corresponding to the second premolar, first molar, and second molar teeth. Notably, the consideration of the mandibular canal was omitted. A comparison was then conducted between the partially constructed bone model and the virtual mandibular bone model obtained from Complete Anatomy software (3D4Medical, Elsevier) to evaluate the accuracy. Multiple enhancements were implemented on the bone model, which included smoothing out the upper section to alleviate the presence of extensively distorted meshes within that specific area. Upon completion, the resultant bone model exhibited dimensions of 30 mm in length, 20 mm in height, and 8 to 10 mm in width. These dimensions were consistent with those reported in some past numerical studies that had focused on the same regions of interest [21,22]. To address the necessity of simulating bone segments exhibiting different bone qualities, two cortical bone models incorporating different thicknesses were developed. As a result,

guided by the classification framework proposed by Lekholm and Zarb, in conjunction with insights drawn from Demenko's research, a cortical layer with the thickness of 2 and 1 mm was constructed to represent type II and type III bone densities, respectively, as depicted in Figure 1(a).

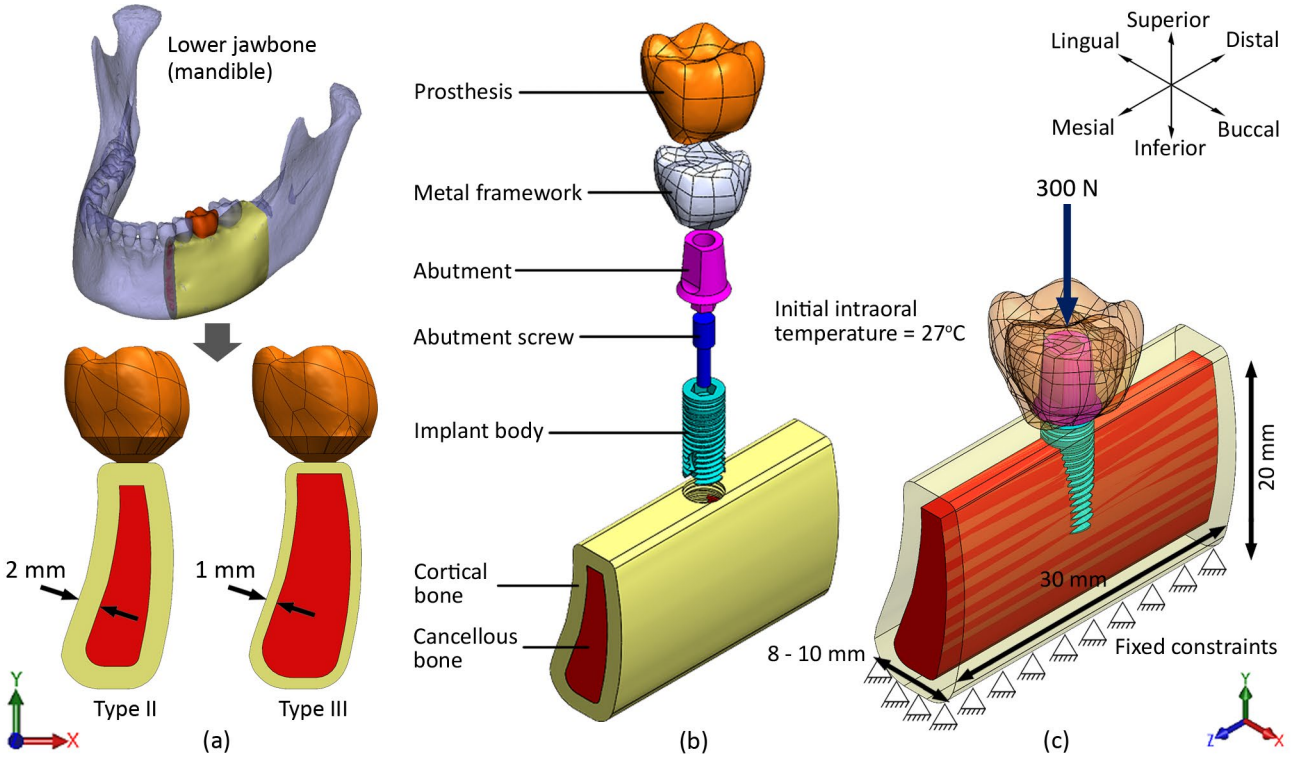

Fig. 1. (a) The thickness of the cortical layer for type II (2 mm) and type III (1 mm) bone qualities (b) Exploded view of implant-bone complex (c) Applied load and boundary condition of the model

Taking into account the presence of the porous body, referred to as cancellous bone, it was modelled as a compact, continuous entity endowed with properties akin to spongy material. The spongy bone was surrounded by the denser outer shell (cortical bone). In order to replicate the implant insertion into the bone, the model omitted the first molar tooth as a representation of a single-tooth restoration, while neglecting the inclusion of the other two adjacent teeth. To represent the prosthesis or crown, a model mirroring the anatomical structure of the first molar's enamel was generated using Boolean operations. Additionally, the framework was constructed by proportionally reducing the dimensions of the prosthesis model by approximately 30%.

2.2 Construction of Three-Dimensional Implant Model

A three-dimensional model, aligning with the specifications of the dual-fit implant (DFI) offered by Alpha-Bio Tec in Petach Tikva, was created for the implant body, abutment, and abutment screw. This modelling process was conducted using SolidWorks 2020, a computer-aided design software by SolidWorks Corp. (Concord, Massachusetts, USA). The implant body possessed a diameter of 3.75 mm. For the implant length, five different length values ranging from 4, 6, 10, 13 to 15 mm were investigated. The consideration of these dimensions was based on the typical lengths of implants observed in clinical practices. The implant-abutment interface was structured with an internal hexagonal connection, and the thread configuration of the implant was designed in the form of a V-shaped pattern. The implant body was designed as a unified structure, attached to the abutment, and stabilization was achieved using a securing screw. The abutment stands at a height of 3.5 mm,

while the screw spans 2.2 mm in width and 8 mm in length. Using SolidWorks, the models for all components of the implant were meticulously developed using a range of intrinsic geometry tools, such as extrusion, revolution, sweeping, and lofting. Rigorous validation was performed by comparing the final 3-D models with the documented dimensions and tolerances provided in the implant manufacturer's catalogue, thereby substantiating the accuracy of the models. In Figure 1(b), an exploded view defines the implant parts alongside the bone models for enhanced visual clarity.

2.3 Simulation of Implant Placement in Bone

In the SolidWorks software, all designed bone and implant component models underwent transformation into solid geometries to establish the precise implant placement within the bone structure. This process adhered closely to the recommended surgical procedures outlined by the Brånemark System®. The selected approach involved bone-level implant placement, where alignment was achieved by ensuring parallelism between the implant platform's flat surface and the uppermost cortical bone surface, maintaining consistent elevation. This alignment was integral to ensuring optimal prosthesis orientation. To create a 3.75-mm wide bone bed, the "Combine" feature, accessible through the "Subtract" tool, was employed to successfully implement this geometric modification. Figure 2 shows the configuration of all implant lengths in the bone model.

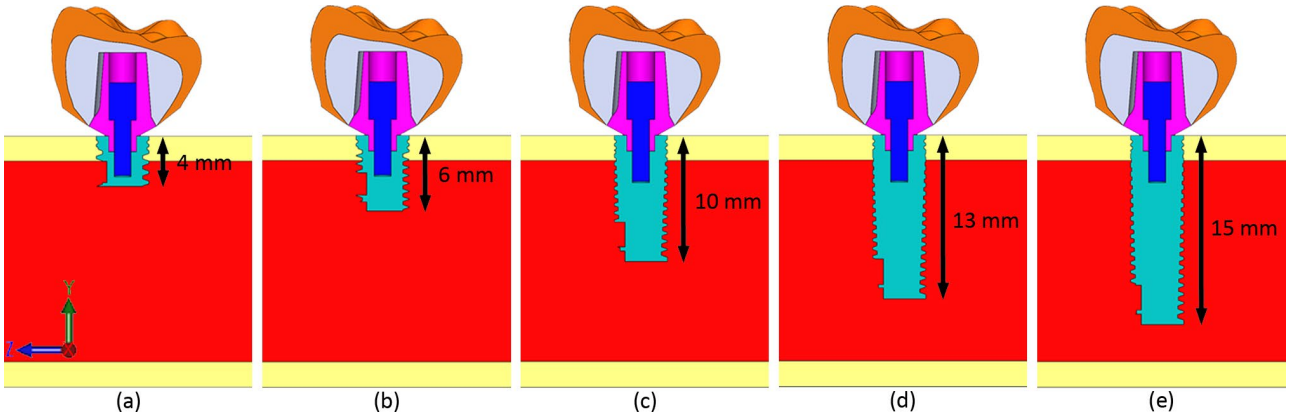

Fig. 2. Five different implant lengths analysed in the study, (a) 4 mm, (b) 6 mm, (c) 10 mm, (d) 13 mm, and (e) 15 mm

2.4 Modelling of Contact Interaction

The connection between the implant body and the bone structures was hypothesized to represent an ideal bonded link, indicating full osseointegration. This concept has been commonly supported in various previous in-vitro studies. This approach entailed the utilization of the direct contact method to preclude any potential relative motion at the interface. Similarly, this contact modelling was extended to the interfaces between the cortical and cancellous bone regions. Conversely, the simulation of interaction between implant and prosthetic parts involved the utilization of a friction coefficient (μ) set at 0.3 [23]. The selected approach to handle interaction at these interfaces involved utilizing the Augmented Lagrange method, which was under the automatic control of the software. Instances of contact were detected at the Gauss integration point.

2.5 Assignment of Material Properties

Anisotropic properties were attributed to the bone models, while the implant components were designated with isotropic characteristics. The structural strength of the bone is intricately linked to the organization of collagen fibers within its structure. Notably, the elastic modulus of the mandibular cortical layer demonstrates its minimum value along the transverse corono-apical or bucco-lingual direction (90°), while its highest magnitude is observed along the longitudinal mesio-distal direction (0°). Numerous computational studies have placed emphasis on incorporating anisotropic properties of biological tissues to enhance the reliability of outcomes [8,24]. Table 1 contains a list of the material properties utilized for characterizing all finite element models employed in the analyses.

Table 1
The material characteristics specific to each finite element model

Material	Model	Elastic Modulus, E (GPa)	Poisson's Ratio, v	Shear Modulus, G (GPa)	References
Ti-6Al-4V	Abutment, abutment screw & implant body	113.8	0.342	-	Yalçın *et al.,* [21]
Feldspathic porcelain	Prosthesis	82.8	0.35	-	Tekin *et al.,* [25]
CoCr alloy	Framework	218	0.33	-	Elias *et al.,* [26]
Cortical bone (type II and III)	-	E_x = 17.9 E_y = 12.5 E_z = 26.6	v_{yz} = 0.31 v_{xy} = 0.26 v_{xz} = 0.28	G_{yz} = 5.3 G_{xy} = 4.5 G_{xz} = 7.1	Robau-Porrua *et al.,* [8]
Cancellous bone (type II and III)	-	E_x = 1.148 E_y = 0.021 E_z = 1.148	v_{yz} = 0.055 v_{xy} = 0.003 v_{xz} = 0.322	G_{yz} = 0.068 G_{xy} = 0.068 G_{xz} = 7.100	Robau-Porrua *et al.,* [8]

2.6 Applied Loads and Boundary Conditions

Within this study, two distinct loading scenarios were considered: occlusal loading and screw pretension. In order to mimic the chewing action, a dynamic occlusal force of 300 N was exerted onto the upper surface of the prosthesis, in alignment with the implant's longitudinal axis [21]. The force was applied vertically along the *y*-axis (in the downward direction) to simulate the dominant effect of occlusal activity. Concurrently, for the pretension scenario, a 20 N force was directed onto the external surface of the abutment screw [21]. An initial temperature of 27°C was defined for the environment inside the mouth. Regarding the structural boundary conditions, fixed constraints were applied to the lower plane of the cortical bone model, preventing any form of translational and rotational displacement in the *x*, *y*, and *z* directions [21]. Figure 1(c) graphically illustrates the loading and boundary conditions used in the analysis.

2.7 Verification of Finite Element Model

The validity of the finite element analysis (FEA) outcomes necessitates their independence from purely numerical factors. Therefore, conducting a mesh convergence test stands as a pivotal aspect. Preceding the convergence test, all models were converted into solid tetrahedral elements within the ANSYS software platform (ANSYS Inc., Houston, TX, USA), adopting a four-node element type while accommodating three degrees of freedom. To execute the mesh convergence test, the model was subjected to incremental variations in mesh density, encompassing differing numbers of elements. The approximated mesh compositions of Tet-A, Tet-B, Tet-C, Tet-D, Tet-E, and Tet-F were

190,000, 260,000, 410,000, 750,000, 1,083,000, and 1,690,000 elements, respectively. The automatic solid meshing function within ANSYS software was applied for this purpose. The focal point of the analysis lay in the maximum principal stress outcomes observed within the bone structure, surveyed across all iterations of the convergence test. The findings indicated a marginal discrepancy in stress values between the coarser and the more refined models. Convergence was observed in the tetrahedral model, with the most substantial alteration being a 2.7% shift following a single refinement, which encompassed around 400,000 nodes and 260,000 elements. Figure 3 illustrates a graphical representation of the distribution of maximum principal stress value within the bone structure. The figure also shows mesh configurations before refinement (Tet-A) and after a single refinement iteration (Tet-B).

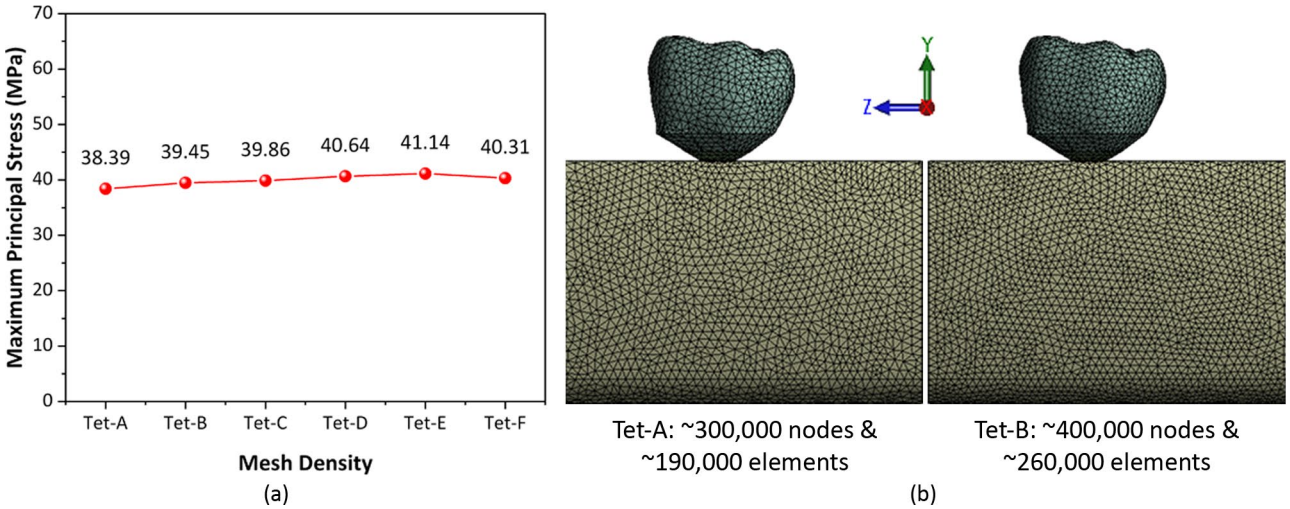

Fig. 3. (a) Various mesh densities were analysed for the maximum principal stress experienced within the bone (b) The mesh distribution was compared between Tet-A (initial) and Tet-B (after a single refinement)

For verification purposes, the newly proposed finite element model underwent a comparison with prior studies that examined analogous implant sites and restoration scenarios. The same pre-processing parameters used in those studies were duplicated, with the exception of variations in model geometry. This comparative analysis was focused on the evaluation of the specific response data type utilized in each selected study, namely, the equivalent von Mises stress (MPa) within the bone structure. The findings demonstrated a high degree of consistency between the stress levels observed in our model and those reported in previous studies, as evidenced by minimal disparities (summarized in Table 2). The percent differences were 35.4% and 11.8% for the comparison made with the work by Yalçın *et al.,* and Schwitalla *et al.,* respectively. The consistency in the results was attained because comparable pre-processing configurations were applied in the analyses.

Table 2
Comparison of the highest bone stress value between the literature and our proposed models

Previous Works	Literature Results	Our Results
Yalçın *et al.,* [21]	20.93 MPa	29.93 MPa
Schwitalla *et al.,* [22]	17.00 MPa	19.13 MPa

3. Results

The analysis results were showcased by highlighting critical values associated with various key biomechanical responses, such as maximum principal stress (for bones), equivalent von Mises stress (for the implant body), maximum principal strain (in bones), and overall deformation (in the implant body-abutment complex). To enhance clarity, colour contour plots were employed, with red denoting elevated stress, strain, or deformation values, while blue indicated lower magnitudes. A summarized overview of the analysis results for each specific scenario was presented in Table 3.

Table 3
The stress, strain, and total deformation magnitudes obtained in all cases

Implant length (mm)	Maximum principal stress (MPa)		Equivalent von Mises stress (MPa)		Maximum principal strain		Total deformation (μm)	
	Type II	Type III	Type II	Type III	Type II	Type III	Type II	Type III
4	87.86	80.50	505.32	500.45	0.006828	0.054250	0.1458	0.1754
6	49.14	214.74	580.69	518.34	0.005270	0.047960	0.1415	0.1694
10	50.17	89.50	625.35	558.63	0.006447	0.021678	0.1362	0.1555
13	36.66	2128.90	559.19	2186.70	0.003413	0.106550	0.1374	0.1492
15	77.75	95.75	571.54	566.05	0.003328	0.022701	0.1348	0.1495

Figure 4 shows that the application of longer implants, in general, led to reduced bone stress levels in type II bone (87.86 to 36.66 MPa), in comparison to those observed in type III bone. In the case of type III bone, there is observable evidence of increasing bone stress values with the utilization of longer implants (80.5 to 2128.9 MPa). However, the extent of the increase displayed irregular consistency. Longer implants exhibited a tendency to reduce stress concentration within the bone structure that spanning from the coronal to the apical region. Upon interpreting the outcomes in terms of varying bone quality classifications, noticeable variations were evident in the levels of bone stress. Type III bone exhibited higher stress values compared to type II bone across nearly all implant lengths. This observation is consistent with the pattern of stress distribution, wherein type III bone showcased a more pronounced region of high stress intensity compared to type II bone. Irrespective of variations in bone qualities, the region of the bone surrounding the implant's coronal area demonstrated elevated stress accumulation in contrast to the apical region.

For the stress results in the implant body, it was noted that the stress value generally increased as the longer implants were used for type II bone, ranging from 505.32 to 625.35 MPa. A similar pattern emerged in type III bone, where the stress magnitudes surged from 500.45 to 2186.7 MPa (shorter to longer implants). The highest stress level was recorded in the implant length of 10 mm and 13 mm for type II and type III bones, respectively. When evaluating the stress values across implant lengths, the implant body in type II bone consistently showed greater stresses compared to type III bone, except at the implant length of 13 mm. As depicted in Figure 5, the stress patterns predominantly spread in the mesio-distal axis and exhibited significant concentration at the junction between the abutment and the implant. This concentration of stress reduced and led to a lesser formation of focused region when the implant length was increased in both types of bone. The least prominent area of stress concentration within the implant body was closely linked to the application of shorter implants.

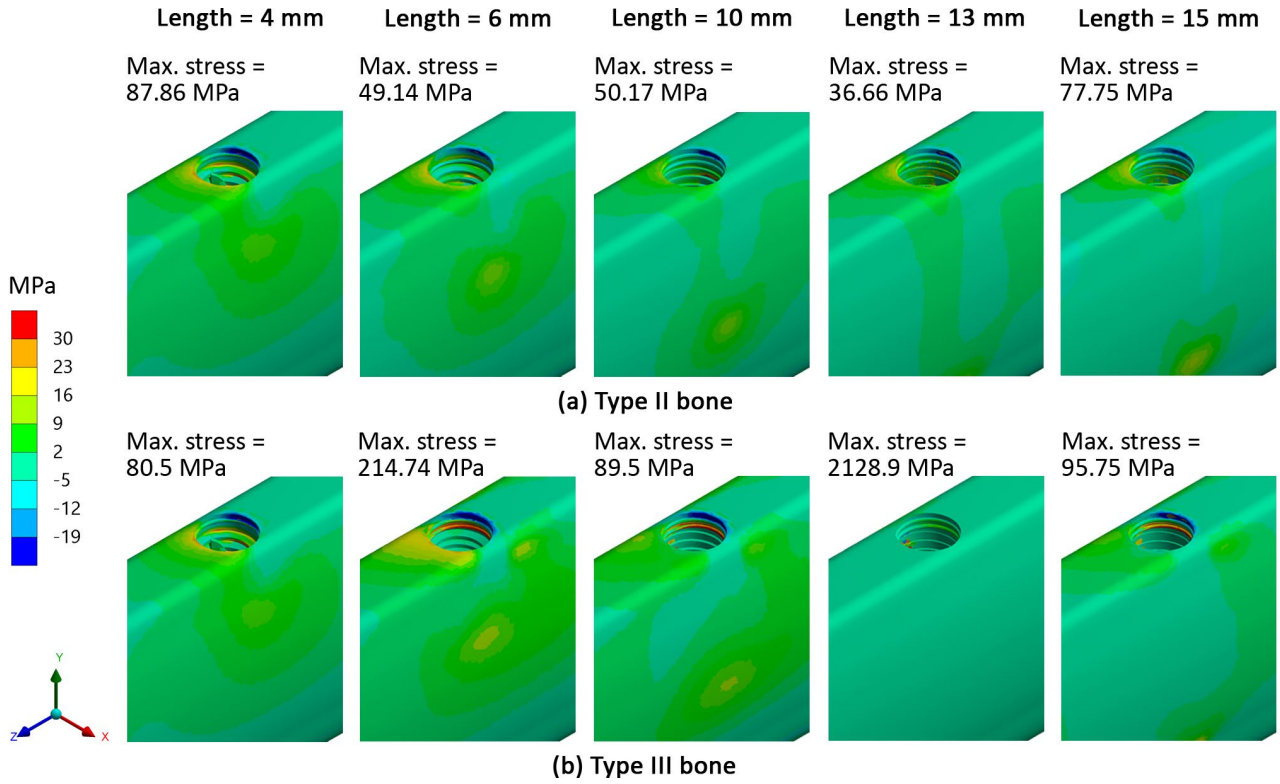

Fig. 4. Contour maps illustrating the maximum principal stress within the bones for different implant lengths under (a) type II and (b) type III bone qualities

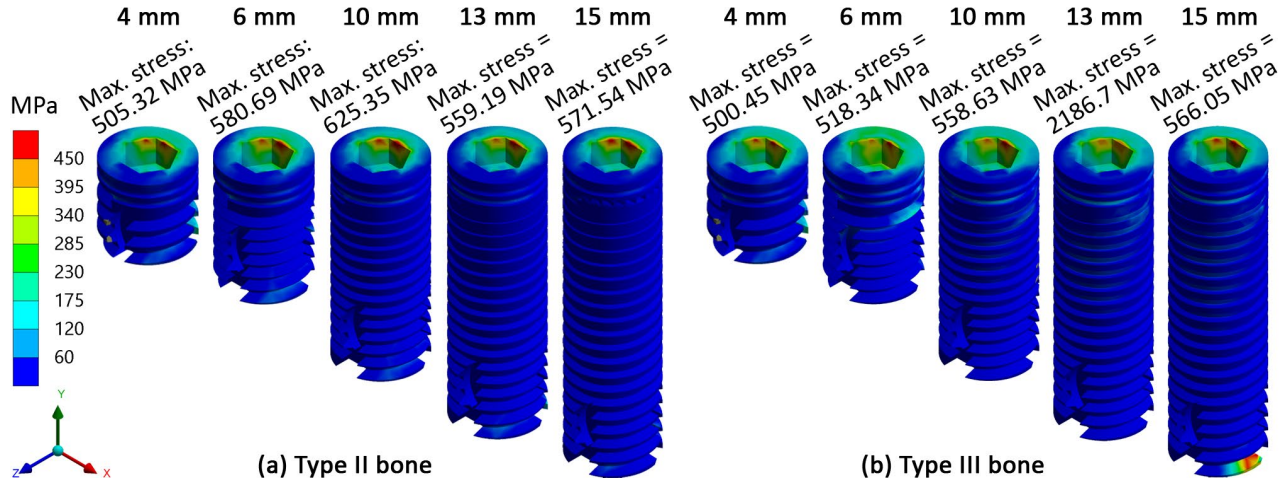

Fig. 5. Contour maps illustrating the maximum equivalent von Mises stress within the implant body for different implant lengths under (a) type II and (b) type III bone qualities

The configuration of the implant body with the increased length seems to have generally resulted in the decreased bone strain values for both type II (0.006828 to 0.003328) and type III bones (0.05425 to 0.021678). However, a considerable spike of strain (0.006447 and 0.10655) being seen in 10-mm and 13-mm implants, under type II and type III bones, respectively. Overall, the levels of maximum bone strain generated were significantly greater in type III bone when compared to type II bone. The areas of elevated strain were mainly focused on the coronal part of the connection between the implant body and the bone, and they extended towards the surrounding areas (Figure 6). The apical section of the bone appeared to exhibit less variation in strain compared to the coronal section, and the region of strain concentration was reduced as the implant length increased.

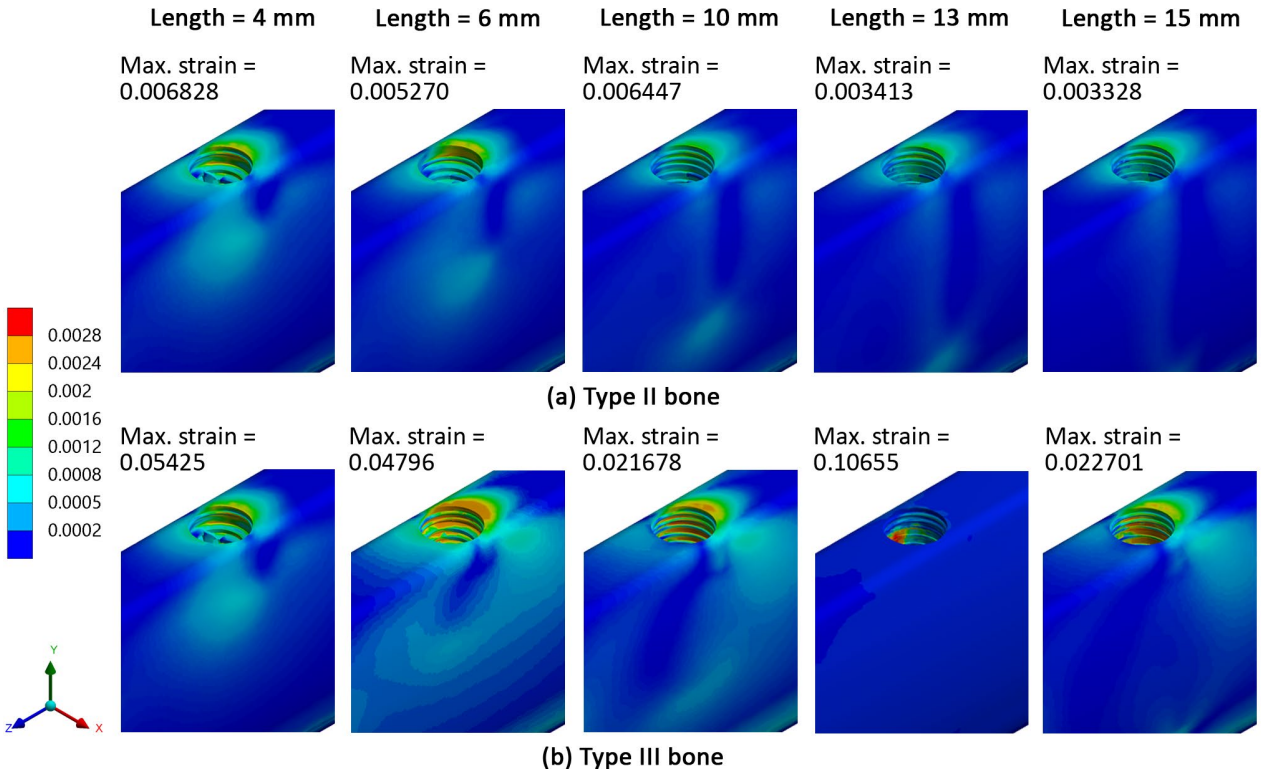

Fig. 6. Contour maps illustrating the maximum principal strain within the bones for different implant lengths under (a) type II and (b) type III bone qualities

The extent of displacement in the implant-abutment assembly (Figure 7) showed a predominantly decreasing trend in relation to implant length. This decrease was particularly notable when using longer implants in type II (from 0.1458 mm to 0.1348 mm) and type III bones (from 0.1754 mm to 0.1492 mm). The minimum value of displacement was recorded for 15-mm implant: 0.1348 mm and 13-mm implant: 0.1492 mm in type II and type III bones, respectively. In comparison, the implant-abutment complex resulted in a higher deformation in type III bone, while the reverse was noticed in type II bone. A significant zone of concentrated displacement developed, starting from the abutment at the upper part and spreading towards the lower end of the implant body. This indicates a minor inclination for deformation in the intermediate and lower parts of the assembly in both groups of bone quality.

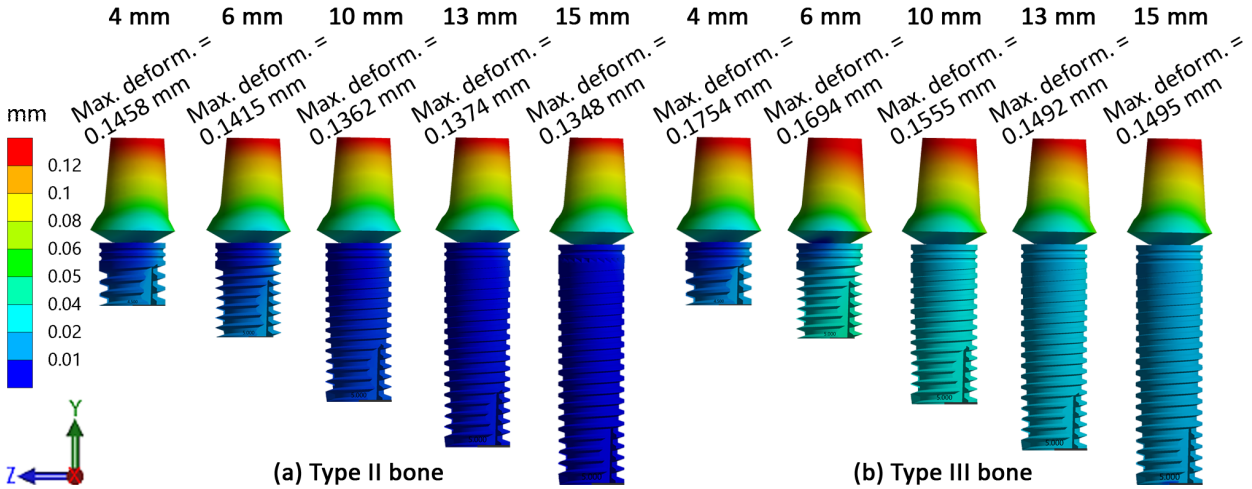

Fig. 7. Contour maps illustrating the total deformation of the implant-abutment complex for different implant lengths under (a) type II and (b) type III bone qualities

4. Discussions

This study is motivated by the occurrence of technical dental implant failures attributed to an unclear understanding of implant macrogeometry and bone conditions under physiological loading. The primary objective is to analyse the impact of varying implant lengths and bone qualities through 3-D FEA. The novelty of this research lies in establishing a relationship between implant length and bone quality, providing potential benefits for clinical practitioners in both pre- and post-treatment phases for patients. The length of the implant is determined by the distance from the implant's platform to its apex. The selection of an appropriate implant length involves a comprehensive evaluation of several factors, including patient-specific considerations and the anatomical characteristics of the target site. Of particular significance is the initial establishment of contact between the bone tissue and the implant body, a factor that significantly impacts the functional surface area. This pivotal parameter is closely tied to the inherent bone density, a classification system denoted as type I, II, III, and IV. Type I bone exhibits a higher potential, with the potential for achieving approximately 80% bone-implant contact, whereas type II, III, and IV designations are associated with progressively lower percentages of such contact [11]. In addition to considerations regarding bone quantity and quality, the proficiency of the clinician in managing novel implant designs can exert a discernible impact on the resultant treatment outcomes.

A lower level of stress was expected within the bone when longer implants were used in type II bone with the lowest value was recorded for the 13-mm-long implant. Nevertheless, an unexpected situation was found when the bone stress magnitude was generally increased as the longer implants applied in type III bone. This finding is probably associated with the total implant surface area. In type II bone, an extension in the implant length corresponds to an increase in the total area of bone-to-implant contact. According to Lee *et al.,* the increase in the total contact surface may subsequently improving the primary stability and promising a greater implant survival rate [10]. This is also in agreement with Robau-Porrua *et al.,* who stated that extending the implant length could lead to a decrease in stress levels within both cortical and cancellous bones [8]. For the case of implant in type III bone, a lower contact surface was generated between the implant and the bone particularly at the cortical bone structure as the thickness of that structure is considerably lower than that in type II bone. It seems that the configuration of the cortical bone is important in affecting the structural integrity of a dental implant in the bone, consistent with that reported in past studies [8, 27]. Irrespective of bone qualities, the distribution of high stress concentration was primarily observed in the cortical layer rather than in the cancellous bone. This seems contradict with some previous findings that stated the implant length is more responsible for mechanical responses at the cancellous bone compared to the cortical layer [28,29]. Although the bone-to-implant contact surface area was increased in both bone types by increasing the length of the implant, the influence of geometrical factor of the cortical bone (thickness) could not totally be disregarded as the level of bone stresses recorded was significantly affected. The peak values for bone stress all remained below the cortical bone's strength threshold of 170 MPa [30], except for those under 6-mm (214.74 MPa) and 13-mm (2128.9 MPa) implants in type III bone.

The present results also exhibited that the increase in the implant length had generally increased the mechanical stress value and corresponding stress intensity region within the implant body for both groups of bone quality which contrasted to the bone stress results. It is noteworthy that a longer extension of an implant body could increase the bending moment generated. This could explain the increasing value of implant stress recorded in the analyses from the shorter to longer implants. As indicated by Chrcanovic *et al.,* each additional millimeter in implant length resulted in a 22.3% rise in the likelihood of experiencing a fracture [3]. Also, based on previous findings, recommending shorter

implants emerges as a dependable alternative for addressing posterior mandible concerns related to mandibular canal violation [31,32]. The shorter implants not only prevent bone heating during site preparation but also streamline treatment planning, shorten the overall treatment period, and incur reduced costs. The implants in type II bone mostly promoted greater stress levels than those in type III bone that probably be due to a better surrounding bony support from the cortical layer. This situation provides an improved structural retention towards the implant body in resisting the imposed occlusal force. The analyses consistently recorded maximum stress values for the implant that remained below the yield strength of the implant material (Ti-6Al-4V), which stands at 880 MPa except the 13-mm-long implant (2186.7 MPa) in type III bone. The lower stress magnitudes than the yield strength of the material may indicate a low risk of implant failure. Our results demonstrated that significant stress concentration exists in the implant neck region, at the implant-abutment connection. This agrees with the findings in prior research [33,34].

For bone strain, the outcomes seemed to be opposite with the implant stress result wherein the shorter implant being the main influencing factor. The shorter implants had resulted in high strain concentration at the top region of the bone-implant interface in type II and type III bones. Besides, the values of bone strain in type III bone were considerably higher than those in type II bone. The finding is probably due to the limited region for the bone structure to deform corresponding to the shorter implant models used. On the contrary, longer implants possess a larger embodiment area to the attached bones to compensate the deformation, thus resulting in low deformation. The type III bone appeared to offer more bone strains which could be because of low resistance (thinner cortical layer) towards the loading applied. To relate the bone strain data obtained to bone reactions, Frost's mechanostat theory is adopted [35,36]. Our findings revealed that most of bone strain values generated were greater than 4,500 μ, which signifying pathological overload. Only three bone strains by 13- and 15-mm implants under type II bone showed the values lower than 3,500 μ, indicating physiological overload. The finding somehow does not correspond well with clinical situations. It is suggested that different strain threshold could be adopted to elucidate the bone strain surrounding the dental implant body.

As the length of the implant body increased, there appeared to be a reduction in the displacement of the implant-abutment assembly in both bone types as the retentive strength of the implant body increased. This has accordingly reduced the tendency of the implant to dislocate from its original position in sustaining the loading. Moreover, it may also be associated with the increased total contact surfaces of the implant to the bone, as explained earlier, that securing more placement of the longer implants. Like the bone stress and strain recorded, type III bone was observed to highly affect the displacement of the assembly compared to type II bone. Overall, all the displacement magnitudes of the implant-abutment complex in type II bone were in the range of 50 – 150 μm and the reverse was observed for most of the cases in type III bone. Deviation beyond this range has the potential to detrimentally affect the bone-implant interface, primarily attributed to the development of fibrous tissues [37].

In light of the substantial findings, there exist opportunities for further enhancement. These could encompass the introduction of tilting forces during implant loading, exploration of diverse implant body materials, and an alternative approach to extracting implants from the osseous socket. Nevertheless, this study does have certain limitations: (1) the simulated occlusal loading was localized to a specific point or node; (2) the gingival soft tissue model was not considered; and (3) the evaluation was restricted to the restoration of the mandibular first molar, thus confining the applicability of the results solely to this specific group of teeth. The current observation cannot be directly extended to actual clinical scenarios, but it does have the potential to reveal distinctions in biomechanical responses through computational modelling. In order to substantiate and

authenticate the analytical outcomes in line with regulatory benchmarks, it is essential to conduct *in vitro* and/or *in vivo* clinical investigations. This study disproved the initial null hypothesis. Our findings effectively highlighted that variation of both implant length and bone quality significantly influence biomechanical responses.

5. Conclusion

The conclusions drawn from simulated loadings and non-linear analysis findings align as follows. The longer implants demonstrated a decreased and increased stress magnitudes within the bone in type II and type III bones, respectively, compared to the shorter implants. Whilst, the stress within the implant body was generally increased as the longer implants used in both bone types. Also, irrespective of bone qualities, longer implants tended to result in decreased levels of bone strain and reduced overall deformation within the implant-abutment assembly when compared to their shorter counterparts. Of all findings evaluated, type III bone exhibited a more significant detrimental effect on the biomechanical behaviours of dental implant and surrounding bone except for the implant stresses under the applied physiological loading. Anticipated outcomes of enhanced preoperative implant treatment planning concerning implant geometry and bone condition status are expected to yield dental implants that exhibit optimal performance, subsequently reducing the potential for implant failure.

Acknowledgement

The authors would like to acknowledge the support from Fundamental Research Grant Scheme (FRGS) under a grant number of FRGS/1/2020/TK0/UNIMAP/03/2 from the Ministry of Higher Education Malaysia. The authors reported no conflicts of interest related to this study.

References

[1] Pal, Tamal Kanti. "Fundamentals and history of implant dentistry." *Journal of the International Clinical Dental Research Organization* 7, no. Suppl 1 (2015): S6-S12. https://doi.org/10.4103/2231-0754.172933

[2] Agustín-Panadero, Rubén, Raquel León-Martínez, Carlos Labaig-Rueda, Joan Faus-López, and Maria Fernanda Solá-Ruíz. "Influence of Implant-Prosthetic Connection on Peri-Implant Bone Loss: A Prospective Clinical Trial with 2-Year Follow-up." *International Journal of Oral & Maxillofacial Implants* 34, no. 4 (2019). https://doi.org/10.11607/jomi.7168

[3] Chrcanovic, Bruno Ramos, Jenö Kisch, Tomas Albrektsson, and Ann Wennerberg. "Factors influencing the fracture of dental implants." *Clinical implant dentistry and related research* 20, no. 1 (2018): 58-67. https://doi.org/10.1111/cid.12572

[4] Stoichkov, Biser, and Dimitar Kirov. "Analysis of the causes of dental implant fracture: A retrospective clinical study." *Quintessence International* 49, no. 4 (2018): 279-286. https://doi.org/10.3290/j.qi.a39846

[5] Naveau, Adrien, Kouhei Shinmyouzu, Colman Moore, Limor Avivi-Arber, Jesse Jokerst, and Sreenivas Koka. "Etiology and measurement of peri-implant crestal bone loss (CBL)." *Journal of clinical medicine* 8, no. 2 (2019): 166. https://doi.org/10.3390/jcm8020166

[6] Gupta, Swati, Hemant Gupta, and Amrit Tandan. "Technical complications of implant-causes and management: A comprehensive review." *National journal of maxillofacial surgery* 6, no. 1 (2015): 3-8. https://doi.org/10.4103/0975-5950.168233

[7] Kunjappu, Jimly, Mathew, Vinod, Abdul Kader, M, Kuruniyan, Mohammed, Mohamed Ali, Ahamed, and Shamsuddin, Shaheen. "Fracture of dental implants: An overview." *International Journal of Preventive and Clinical Dental Research* 6, no. 1 (2019): 21-23. https://doi.org/10.4103/inpc.inpc_27_19

[8] Robau-Porrua, Amanda, Yoan Pérez-Rodríguez, Laura M. Soris-Rodríguez, Osmel Pérez-Acosta, and Jesús E. González. "The effect of diameter, length and elastic modulus of a dental implant on stress and strain levels in peri-implant bone: A 3D finite element analysis." *Bio-medical materials and engineering* 30, no. 5-6 (2020): 541-558. https://doi.org/10.3233/BME-191073

[9] Ishak, Muhammad Ikman, Daud, Ruslizam, Ibrahim, Ishak, Mat, Fauziah, and Mansor, Nurul Najwa. "A review of factors influencing peri-implant bone loss." *AIP Conference Proceedings* 2347, no. 1 (2021): 020293. https://doi.org/10.1063/5.0051600

[10] Lee, Jae-Hoon, Val Frias, Keun-Woo Lee, and Robert F. Wright. "Effect of implant size and shape on implant success rates: a literature review." *The Journal of prosthetic dentistry* 94, no. 4 (2005): 377-381. https://doi.org/10.1016/j.prosdent.2005.04.018

[11] Misch, C. E., J. T. Strong, and M. W. Bidez. "Chapter 15-Scientific rationale for dental implant design." *Mosby, St. Louis* (2015). https://doi.org/10.1016/B978-0-323-07845-0.00015-4

[12] Ishak, Muhammad Ikman, and Mohammed Rafiq Abdul Kadir. *Biomechanics in dentistry: evaluation of different surgical approaches to treat atrophic maxilla patients*. Springer Science & Business Media, 2012. https://doi.org/10.1007/978-3-642-32603-5_4

[13] Ishak, Muhammad Ikman, Mohammed Rafiq Abdul Kadir, Eshamsul Sulaiman, and Norhayaty Abu Kassim. "Effects of different zygomatic implant body surface roughness and implant length on stress distribution." In *2010 IEEE EMBS Conference on Biomedical Engineering and Sciences (IECBES)*, pp. 210-215. IEEE, 2010. https://doi.org/10.1109/IECBES.2010.5742230

[14] Ishak, Muhammad Ikman, Aisyah Ahmad Shafi, M. U. Rosli, C. Y. Khor, M. S. Zakaria, Wan Mohd Faizal Wan Abd Rahim, and Mohd Riduan Jamalludin. "Biomechanical evaluation of different abutment-implant connections–a nonlinear finite element analysis." In *AIP Conference proceedings*, vol. 1885, no. 1. AIP Publishing, 2017. https://doi.org/10.1063/1.5002258

[15] Quanjin, Ma, Merzuki, M. N. M., Rejab, M. R. M., Sani, M. S. M., and Bo, Zhang. "Numerical investigation on free vibration analysis of kevlar/glass/epoxy resin hybrid composite laminates." *Malaysian Journal on Composites Science and Manufacturing* 9, no. 1 (2022): 11-21. https://doi.org/10.37934/mjcsm.9.1.1121

[16] Rosli, M. U., Muhammad Ikman Ishak, Mohd Riduan Jamalludin, C. Y. Khor, M. A. M. Nawi, and AK Mohamad Syafiq. "Simulation-based optimization of plastic injection molding parameter for aircraft part fabrication using response surface methodology (RSM)." In *IOP conference series: materials science and engineering*, vol. 551, no. 1, p. 012108. IOP Publishing, 2019. https://doi.org/10.1088/1757-899X/551/1/012108

[17] Nawi, M. A. M., Muhammad Ikman Ishak, M. U. Rosli, Nur Musfirah Musa, Siti Nor Azreen Ahmad Termizi, C. Y. Khor, and M. A. Faris. "The effect of multi-staged swirling fluidized bed on air flow distribution." In *IOP Conference Series: Materials Science and Engineering*, vol. 864, no. 1, p. 012194. IOP Publishing, 2020. https://doi.org/10.1088/1757-899X/864/1/012194

[18] Zulkifli, R. M., Nawi, M. A. M., Ishak, M. I., Rosli, M. U., Termizi, S. N. A. Ahmad, Khor, C. Y., and Faris, M. A. "Influence of twisted blades distributor towards low pressure drop in fluidization systems." *Intelligent Manufacturing and Mechatronics* (2021): 703-711. https://doi.org/10.1088/1757-899X/864/1/012194

[19] Islam, Md Saifi Bin, Muhammad Faiz Ahmed, and Abdullah Al Saad. "Numerical Investigation on the Aerodynamic Characteristics of a Wing for Various Flow and Geometrical Parameters." *Malaysian Journal on Composites Science and Manufacturing* 12, no. 1 (2023): 13-30. https://doi.org/10.37934/mjcsm.12.1.1330

[20] Khan, Umair Ahmad, Hamid Ullah, and Ahmad Nawaz. "Design and Optimization of Heatsink for an Active CPU Cooler using Numerical Simulations." *Journal of Advanced Research in Fluid Mechanics and Thermal Sciences* 111, no. 2 (2023): 214-224. https://doi.org/10.37934/arfmts.111.2.214224

[21] Yalçın, Mustafa, Beyza Kaya, Nihat Laçin, and Emre Arı. "Three-Dimensional Finite Element Analysis of the Effect of Endosteal Implants with Different Macro Designs on Stress Distribution in Different Bone Qualities." *International Journal of Oral & Maxillofacial Implants* 34, no. 3 (2019). https://doi.org/10.11607/jomi.7058

[22] Schwitalla, A. D., Abou-Emara, M., Spintig, T., Lackmann, J., and Müller, W. D. "Finite element analysis of the biomechanical effects of PEEK dental implants on the peri-implant bone." *Journal of Biomechanics* 48, no. 1 (2015): 1-7. https://doi.org/10.1016/j.jbiomech.2014.11.017

[23] Tribst, João Paulo Mendes, Dal Piva, Amanda Maria de Oliveira, Borges, Alexandre Luiz Souto, and Bottino, Marco Antonio. "Influence of socket-shield technique on the biomechanical response of dental implant: Three-dimensional finite element analysis." *Computer Methods in Biomechanics and Biomedical Engineering* 23, no. 6 (2020): 224-231. https://doi.org/10.1080/10255842.2019.1710833

[24] Tretto, Pedro Henrique Wentz, Mateus Bertolini Fernandes Dos Santos, Aloisio Oro Spazzin, Gabriel Kalil Rocha Pereira, and Atais Bacchi. "Assessment of stress/strain in dental implants and abutments of alternative materials compared to conventional titanium alloy—3D non-linear finite element analysis." *Computer Methods in Biomechanics and Biomedical Engineering* 23, no. 8 (2020): 372-383. https://doi.org/10.1080/10255842.2020.1731481

[25] Tekin, S, Değer, Y, and Demirci, F. "Evaluation of the use of PEEK material in implant-supported fixed restorations by finite element analysis." *Nigerian Journal of Clinical Practice* 22, no. 9 (2019): 1252-1258. https://doi.org/10.4103/njcp.njcp_144_19

[26] Elias, Douglas Máximo, Claudia Scigliano Valerio, Dauro Douglas de Oliveira, Flávio Ricardo Manzi, Elton Gonçalves Zenóbio, and Paulo Isaías Seraidarian. "Evaluation of Different Heights of Prosthetic Crowns Supported by an Ultra-Short Implant Using Three-Dimensional Finite Element Analysis." *The International Journal of Prosthodontics* 33, no. 1 (2020): 81-90. https://doi.org/10.11607/ijp.6247

[27] Petrie, Cynthia S., and John L. Williams. "Comparative evaluation of implant designs: influence of diameter, length, and taper on strains in the alveolar crest: A three-dimensional finite-element analysis." *Clinical oral implants research* 16, no. 4 (2005): 486-494. https://doi.org/10.1111/j.1600-0501.2005.01132.x

[28] Armentia, Mikel, Abasolo, Mikel, Coria, Ibai, and Sainitier, Nicolas. "Effect of the geometry of butt-joint implant-supported restorations on the fatigue life of prosthetic screws." *The Journal of Prosthetic Dentistry* (2022). https://doi.org/10.1016/j.prosdent.2021.12.010

[29] Pirmoradian, Mostafa, Hamed Ajabi Naeeni, Masih Firouzbakht, Davood Toghraie, and Reza Darabi. "Finite element analysis and experimental evaluation on stress distribution and sensitivity of dental implants to assess optimum length and thread pitch." *Computer methods and Programs in Biomedicine* 187 (2020): 105258. https://doi.org/10.1016/j.cmpb.2019.105258

[30] Valera-Jiménez, J. F., Burgueño-Barris, G., Gómez-González, S., López-López, J., Valmaseda-Castellón, E., and Fernández-Aguado, E. "Finite element analysis of narrow dental implants." *Dental Materials* 36, no. 7 (2020): 927-935. https://doi.org/10.1016/j.dental.2020.04.013

[31] Nielsen, H. B., Schou, S., Isidor, F., Christensen, A. E., and Starch-Jensen, T. "Short implants (≤8mm) compared to standard length implants (>8mm) in conjunction with maxillary sinus floor augmentation: A systematic review and meta-analysis." *International Journal of Oral and Maxillofacial Surgery* 48, no. 2 (2019): 239-249. https://doi.org/10.1016/j.ijom.2018.05.010

[32] Leighton, Yerko, Carpio, Luis, Weber, Benjamin, Dias, Fernando Jose, and Borie, Eduardo. "Clinical evaluation of single 4-mm implants in the posterior mandible: A 3-year follow-up pilot study." *The Journal of Prosthetic Dentistry* 127, no. 1 (2022): 80-85. https://doi.org/10.1016/j.prosdent.2020.06.039

[33] Liu, Chaowei, Yifeng Xing, Yan Li, Yanjun Lin, Jianghan Xu, and Dong Wu. "Bone quality effect on short implants in the edentulous mandible: a finite element study." *BMC Oral Health* 22, no. 1 (2022): 139. https://doi.org/10.1186/s12903-022-02164-8

[34] Niroomand, Mohammad Reza, and Masoud Arabbeiki. "Implant stability in different implantation stages: Analysis of various interface conditions." *Informatics in Medicine Unlocked* 19 (2020): 100317. https://doi.org/10.1016/j.imu.2020.100317

[35] Dantas, T. A., Carneiro Neto, J. P., Alves, J. L., Vaz, Paula C. S., and Silva, F. S. "In silico evaluation of the stress fields on the cortical bone surrounding dental implants: Comparing root-analogue and screwed implants." *Journal of the Mechanical Behavior of Biomedical Materials* 104, no. (2020): 103667. https://doi.org/10.1016/j.jmbbm.2020.103667

[36] Matsuzaki, Tatsuya, Ayukawa, Yasunori, Matsushita, Yasuyuki, Sakai, Nobuo, Matsuzaki, Maki, Masuzaki, Tomohiro, Haraguchi, Takuya, Ogino, Yoichiro, and Koyano, Kiyoshi. "Effect of post-osseointegration loading magnitude on the dynamics of peri-implant bone: A finite element analysis and in vivo study." *Journal of Prosthodontic Research* 63, no. 4 (2019): 453-459. https://doi.org/10.1016/j.jpor.2018.10.009

[37] Dorogoy, A., Rittel, D., Shemtov-Yona, K., and Korabi, R. "Modeling dental implant insertion." *Journal of the Mechanical Behavior of Biomedical Materials* 68, no. (2017): 42-50. https://doi.org/10.1016/j.jmbbm.2017.01.021